NUMERICAL ANALYSIS OF VELOCITY PROFILE AND SEPARATION ZONE IN OPEN CHANNEL JUNCTIONS

Waqid Hameed Al-Mussawi
College of Engineering
Karballa University

Abstract

The junction open channel flow is encountered in many hydraulic engineering such as irrigation ditches, wastewater treatment facilities and fish passage conveyance structures. The flow behavior at junction becomes very complex because of the interaction between the branch and main channel, that's cause many complex problems such as local sedimentary, channel scour and sidewall erosion and others. This paper provides detail application of numerical solution (Finite Volume) by FLUENT-2D software in simulation of 90º open channel junction flows. Numerical simulations undertaken in present two dimensional work use Standard k-ε turbulence model. Comparisons have been made between numerical results and measured experimental velocities of Weber et al. (2001), good agreement between the model predictions and experimental measurements have been obtained. The model is then applied to investigate the dimensions of separation zone. The simulation results show that separation zone size increases as the discharge ratio of the upstream main channel to the downstream channel decreases.

التحليل العددي لمخطط السرعة ومنطقة الانعزال في ملتقيات القنوات المفتوحة

واقد حميد الموسوي
كلية الهندسة
جامعة كربلاء

الخلاصة

ان ألتقاء الجريان في القنوات المفتوحة يحدث كثيراً في الهندسة الهايدروليكية،كما في قنوات الري ووسائل معالجة مياه الفضلات ومنشأت تحويل مرور الاسماك في السدود.ان سلوك الجريان في منطقة الألتقاء يصبح معقداً جدا وذلك بسبب التداخل بين مياه القناة الفرعية مع مياه القناة الرئيسية،وهذا يشكل العديد من المشاكل المعقدة مثل حدوث ظاهرة الترسيب الموضعي وتجمع الرسوبيات وتعرية القناة وتأكل الجدران الجانبية للقناة وغيرها .

ان هذا البحث يقدم تطبيق تفصيلي للحل العددي ثنائي الابعاد بطريقة الحجوم المحددة(Finite Volume) بواسطة برنامج (FLUENT) لمحاكاة الجريان في منطقة ألتقاء القنوات المفتوحة وبزاوية 90º .استخدم موديل كي-أبسلون القياسي (Standard k-ε) للجريان المضطرب في تمثيل الجريان.وتم مقارنة نتائج مخططات السرعة اللابعدية من الموديل العددي مع النتائج المختبرية المقاسة من Weber et al.(2001)، ولقد اظهرت المقارنة قبولا جيداً بين النتائج المحسوبة من الموديل والنتائج المختبرية.ثم استخدم الموديل الرياضي للتحري عن أبعاد منطقة الانعزال (Separation zone)، ولقد أظهرت نتائج المحاكاة أن حجم منطقة الانعزال يزداد كلما قلت نسبة تصريف مقدم القناة الرئيسية الى التصريف الكلي في مؤخرة القناة.

Introduction

The junction open channel flows are incredibly complex and interest in environmental and hydraulic engineering. It occurs in many hydraulic structures such as wastewater treatment facilities, irrigation ditch, fish passage conveyance structures and natural river channels. Since we are facing different hydraulic conditions to cause changes in channel alignment, combining of two flows accompanies many complex problems such as local sedimentary, channel scour and sidewall

erosion and others. Some of distinctive characteristics of a junction flow in an open channel are illustrated in Fig.1.A zone of separation immediately downstream of the junction branch channel, a contracted flow region in the main channel due to the separation zone, a stagnation point immediately upstream of the junction, a shear plane developed between the two combining flow, and an increase in depth from the downstream channel to the upstream contributing channels. The zone of separation results due to the momentum of the lateral branch flow causing the main flow to detach at the downstream corner of the junction. Due to a number of important flow phenomena involved, many studies have been conducted to seek the detailed hydrodynamics characteristic of complex junction flow.

Taylor (1944) conducted the first detailed experimental study in an open channel and proposed a graphical solution, which included a trail-and -error procedure.
Best and Reid (1984) show that a well-defined relationship between the dimensions of the separation which form immediately downstream of the junction and the ratio of discharge from the tributary to the total discharge.Weerakoon et al. (1991) examined the three-dimensional flow structure at a junction by means of experimental measurements and a computational model incorporating the k-ε turbulence closure scheme.
Weber et al. (2001) performed an extensive experimental stud of combining flows in 90º open channel for the purpose of providing a very broad data set comprising three velocity components, turbulence stresses, and water surface mappings.
Huang et al. (2002) provided a comprehensive numerical study of combining flows in open channel junction using the 3D turbulence model and validated the model by using the experimental data.
Mao and Wu Rong (2003) provided a numerical simulation of open channel flow in 90º combining junction using Hanjalic-Launder (H-L) modification model to analyze the relative importance of various factors and was compared with laboratory measurements.
A numerical model using finite-element methods was presented by Chong (2006), analysis the open channel junction and a simple comparison with experimental data for velocity profiles were done.
Pirzadeh and Shamloo (2007) provide application of FLUENT -2D&3D software in simulation of lateral intake flows. Comparisons have been made between numerical results and measured experimental velocities for a lateral intake. Comparisons indicate that the 2D simulating captures most experimental trends with reasonable agreement and 3D simulating results have also good accuracy. Shamloo and Pirzadeh (2007) provide the application of FLUENT-2D software in simulation of lateral intake flows, used Standard K-ε turbulence and RSM turbulent models.
In the current study an attempt has been made to model fluid flow through open channel T-junction using FLUENT software and numerical 2-D results for velocity profiles and the dimensions of separation zones with different discharge ratios.

Aim Of Study

The river confluence, which can be defined as a junction of two or more streams, is a frequently found element along a river path. It facilitates to join all streams from many sources over the basin and allows draining them in the form of a river. The river bank erosion and the plunge of the bank due to the lateral flow are critical due to the bank safety. This is well evidenced by the failure of levees at the confluences of many rivers during the floods which resulted serious damages in many countries.
In the design of flood-control channels and fish passage conveyance structures, one of the more important hydraulic problems is the analysis of the flow conditions at open channel junctions. It has recently become more popular to improve the design process using the result from a numerical model study. Applying computational fluid dynamics (CFD) in this field of engineering can improve the final design and accelerate the design process. Also it is importance lies in the fact that the analysis of the junctions is of considerable use to engineers engaged on the design of irrigation systems, drainage systems, channel in sewerage treatment works and other similar projects.

The objective of the present study is the use of 2-D numerical model to predict the velocity profile and dimension of separation zone in the combining flows of open channel junction.

Experimental Data

Velocity profiles obtained from the current numerical model were compared with laboratory experiment results performed by Weber et al. (2001); in their experimental set-up, a sharp-edged,90ºcombining flow flume with horizontal slop as show in (Fig. 2).The upstream main channel, branch channel, and combined tail water flow are denoted as Qm,Qb and Qt, respectively.

The flow ratio q* is defined as the upstream main channel flow Qm to the constant total flow Qt which is equal to $0.170 m^3/s$.The flow conditions tested are listed in Table1.Only q* equal to 0.420 and 0.750 were selected for model simulation.

Weber et al. (2001) presented the results by using normalized distance. All distance were normalized by the channel width, w =0.91m.The non-dimensionalized coordinates are called X*, Y*, and Z* for x/w, y/w, and z/w, respectively.

Numerical Model Description

FLUENT is the CFD solver for choice for complex flow ranging from incompressible (transonic) to highly compressible (supersonic and hypersonic) flows. Providing multiple choices of solver option, combined with a convergence-enhancing multi-grid method, FLUENT delivers optimum solution efficiency and accuracy for a wide range of speed regimes. The wealth of physical models in FLUENT allows you to accurately predict laminar and turbulent flows, various modes of heat transfer, chemical reactions, multiphase flows, and other phenomena with complete mesh flexibility and solution- based mesh adoption (Fluent user guide 2003).

FLUENT solves governing equations sequentially using the control volume method. The governing equations are integrated over each control volume to construct discrete algebraic equations for dependent variables. These discrete equations are linearized using an implicit method. As the governing equations are nonlinear and coupled, iterations are needed to achieve a converged solution.

Conservative form of the Navier-stokes equations using the finite volume method on structured orthogonal, Cartesian coordinate's grid system.

Turbulent flows can be simulated in FLUENT using the standard *k-ε*, LES, RNG, or the Reynolds-stress (RSM) closure schemes.

The model optimizes computational efficiency by allowing the user to choose between various spatial (Second-order upwind, third-order, QUICK) discritization scheme.

In the present study used second order upwind discritization scheme for Momentum, Turbulent kinetic energy and turbulent dissipation rate; used body force weighted discritization scheme for Pressure and SIMPLE algorithm for Pressure-Velocity Coupling Method.

Mathematical Modeling

1- Governing Equations

The governing equations of fluid flow in rivers and channels are generally based on three-dimensional Reynoldes averaged equations for incompressible free surface unsteady turbulent flows as follows (Fluent user guide 2003):

$$\frac{\partial U_i}{\partial t} + U_j \frac{\partial U_i}{\partial x_j} = \frac{1}{\rho}\frac{\partial}{\partial x_j}\left[\left(-P + \frac{2}{3}k\right)\delta_{ij} + v_T\left(\frac{\partial U_i}{\partial x_j} + \frac{\partial U_j}{\partial x_i}\right)\right] \qquad (1)$$

Where:
U_i=velocity in the x_i direction; t = time; ρ=density of flow; P=total pressure; k=turbulently kinetic energy; δ_{ij}=Kronecker delta; v_T=turbulent viscosity; and i, j=1, 2, 3.

There are basically five terms: a transient term and a convective term on the left side of the equation. On the right side of the equation there is a pressure/kinetic term, a diffusive term and a stress term.
In the current study, it is assumed that the density of water is constant through the computational domain. The governing differential equations of mass and momentum balance for unsteady free surface flow can be expressed as (Rodi, 1993):

$$\frac{\partial u_i}{\partial x_i} = 0 \qquad (2)$$

$$\frac{\partial u_i}{\partial t} + u_j \frac{\partial u_i}{\partial x_j} = -\frac{1}{\rho}\frac{\partial P}{\partial x_i} + g_{xi} + \nu\nabla^2 u_i \qquad (3)$$

Where v is the molecular viscosity; g_{xi} is the gravitational acceleration in the x_i direction.
As in the current study, only the steady state condition has been considered, therefore equation (2) to (3) incorporate appropriate initial and boundary conditions deployed to achieve equilibrium conditions.

2- The Standard *K-ε* Model

Turbulent stresses in Reynolds-averaged equations can be closed using any of several exiting turbulence models. No single turbulence model is accepted universally for solving all closes of problems but each model has certain advantages over the others depending on the type and the nature of the flow field to be simulated and the desired accuracy of results (Neary and Odgaard, 1993).
In the standard *k-ε* turbulence model, Reynolds stresses in the Reynolds-average Navier –Stokes equations are modeled by the product of an isotropic eddy viscosity and the local rate of strain. The eddy viscosity is obtained from the product of local turbulence length and velocity scales. The turbulence velocity scale is represented by $k^{1/2}$, where k is the turbulence kinetic energy per unit volume, and the turbulence length scale is determined from ε, the turbulence kinetic energy dissipation rate per unit volume. Both k and ε are derived from transport equations, which are closed by using a number of semi-empirical procedures in which standard constants are employed (Rodi, 1984).
The simplest and most widely used two-equation turbulence model is the *k-ε* model that solves two separate equations to allow the turbulent kinetic energy and dissipation rate to be independently determined.
The turbulence kinetic energy, k, is modeled as:

$$\frac{\partial k}{\partial t} + U_j \frac{\partial k}{\partial x_j} = \frac{\partial}{\partial x_j}\left(\frac{v_T}{\sigma_k}\frac{\partial k}{\partial x_j}\right) + P_k - \varepsilon \qquad (4)$$

Where P_k is given by:

$$P_k = v_T \frac{\partial U_j}{\partial x_i}\left(\frac{\partial U_j}{\partial x_i} + \frac{\partial U_i}{\partial x_j}\right) \qquad (5)$$

$$v_T = c_\mu \frac{k}{\varepsilon^2} \qquad (6)$$

The dissipation of k is denoted ε, and modeled as:

$$\frac{\partial \varepsilon}{\partial t} + U_j \frac{\partial \varepsilon}{\partial x_j} = \frac{\partial}{\partial x_j}\left(\frac{v_T}{\sigma_\varepsilon}\frac{\partial \varepsilon}{\partial x_j}\right) + C_{\varepsilon 1}\frac{\varepsilon}{k}p_k + C_{\varepsilon 2}\frac{\varepsilon^2}{k} \qquad (7)$$

The constants in the k-ε model have the following values: c_μ=0.09, $C_{\varepsilon 1}$=1.44, $C_{\varepsilon 2}$=1.92, σ_k=1.0 and σ_ε=1.30

3- Boundary and Initial Conditions

Appropriate conditions must be specified at domain boundaries depending on the nature of the flow. In simulation performed in the present study, velocity inlet boundary condition used for two inlets (main cannel and branch) at all of runs. Outflow boundary condition used for outlet at all of runs. The length of the main and branch channels were chosen properly with experimental dimensions (Fig.2). The no-slip boundary condition is specified to set the velocity to be zero at the solid boundaries and assumed to be smooth. In simulation performed in the first case of present study, velocity inlet boundary condition is specified, and calculated depend on the discharge ratio. In this case two discharge ratios q*=Qm/Qt equal to 0.420 and 0.750 were used corresponding to the Weber et al. experiments.

In the second case, discharge ratios q*=Qm/Qt equal to 0.083, 0.250, 0.420, 0.583, 0.750 and 0.920 were used.

A finite volume approach is used for the solution of the governing equations. Second order upwind scheme is selected to discretize the governing equations. SIMPLE algorithm is used for pressure-velocity coupling.

It is also important to establish that grid independent results have been obtained. The grid structure must be fine enough especially near the wall boundaries and the junction, which is the region of rapid variation. Various flow computational trials have been carried out with different number of grids in x and y directions. It was found that results are independent of grid size, if at least 5450 nodes are used. Computational mesh is shown in Fig.3.

Results And Discussions

1- Velocity Field

The velocity profiles of turbulent junction open channel flow are of great interest to engineers, particularly in determining the surface resistance to flow which has practical consequences, such as in the estimation of soil erosion and sediment transport in alluvial channels.

In the first case of this paper numerical investigations are performed for evolution of the ability of an available 2D flow solver to cop with the fully turbulent flow in a T-junction. In the **Figures (4)** to **(13)** and **(14)** to **(23)** results of the numerical model are compared with experimental X- velocity profiles in the main channel at 10 non-dimensional locations at x-direction for discharge ratios (q*=0.750 and 0.420) respectively. The velocities are non-dimensionalized with respect to the average downstream, tail water velocity (0.628 m/s). From these **figures**, it can be concluded that results generally have reasonable agreement with measured ones, but at some sections the computed results do not agree very well with those measured, which might be partly due to the three-dimensional effects. Further, due to limitation of two-dimensional numerical model the vertical acceleration is neglected in the current 2D- study. However, both results show the increasing of velocity at outer wall region downstream of the junction.

Statistical analysis of the results obtained was ,also, applied by using chi square test (goodness-of-fit tests) to ensure the previous conclusion.

The chi-square test is the more interesting statistical tests in the engineering field so that it can be used in this analysis. The equation of chi-square known as the following(William,1980):

$$\chi^2 = \sum_{j=1}^{r} \frac{\left(fo_j - fe_j\right)}{fe_j} \qquad (8)$$

Where: fo_j :observed values, fe_j :expected values and *r*: number of rows. The application of results the chi-square equation on the velocities data using level of significance ($\alpha = 0.05$ and $\alpha = 0.1$) is shown in Table (2). It is shown from these analysis, that the chi-square values (χ^2) from equation for all cases less than the chi-square values (χ^2_α) tabulated for level of significance ($\alpha = 0.05$ and $\alpha = 0.1$).From this result we can conclude that all these computed velocities are approximated from the experimental results .

It is found that the FLUENT is an effective tool for predicting flow pattern of the combining flows in open channel junction.

2- Dimension of Separation Zone in the Downstream Main Channel

In the second step at this study, numerical approaches were used to understand flow structure and separation zone at the combining flows in open channel junction.

It was found that the size of separation zone is very much dependent on the discharge ratio. The result showed that the separation zone (recirculation) was observed immediately downstream of the junction due to deflection from outer wall.

Figure (24) shows 2D streamlines plots for discharge ratios (q*=0.083, 0.250, 0.420, 0.583, 0.750 and 0.920). These **figures** elucidate the structure of the combining streams and the zone of flow separation in downstream main channel. The momentum of the lateral branch flow caused the main flow to detach at the downstream corner of the junction. This is more significant for lower (q*) flow condition. As a result, the water depth raised up at the upstream of main channel.

By comparing these **figures**, it is seen that an increase in discharge ratio causes shortening and narrowing of the separation zone. Moreover, the models results show that higher (q*) will take shorter distance downstream from the junction to reach uniform flow condition again.

Figures (25) and **(26)** present the predicted variation of non-dimensional maximum width (S_w) and length (S_L) of separation zone in the main channel respectively, for different discharge ratios.

Results indicate that both length and width of the separation zone decrease with increasing discharge ratio. Separation zone reduces the effective width of the channel. Separation zone can be defined as the area of reduced pressure and re-circulating fluid with low velocities; therefore it has a strong sediment deposition potential in which sediment particles enter the main channel. It can be seen that for a lower discharge ratio, more than 25% of the downstream main channel width is occupied by the recirculation zone.

Fig.27. shows that the contraction coefficient Cc, (Cc=effective width of D/S main channel (w-S_w)/width of main channel (w)), increases linearly as discharge ratio increases. This indicates that a smaller branch discharge Qb results in a small effective width in the recirculation region of the D/S main channel.

The ratio of maximum width (S_w) and length (S_L) of the separation zone shown in Fig.28.This ratio increased in general as discharge ratio increased. The values of (S_w/S_L) range closely around mean value of (0.18); this value was very closely from the mean value (0.19) which calculated by Best and Reid (1984).

Summary And Conclusions

In this study the velocity components and dimensions of separation zone at the downstream main channel for combining flows in a 90°, sharp-edged, rectangular open channel junction formed by channels of equal width are obtained on the basis of numerical studies. It was found the size of separation zone is very much dependent on the discharge ratio. In all cases, the results showed an increase in discharge ratio causes shorting and narrowing of the separation zone.

The numerical simulation models results show that higher discharge ratio will take shorter distance downstream from the junction to reach uniform flow condition again. So, the contraction coefficient increases with the increase in the discharge ratio.

References

Best, J. L. and Reid, I. (1984), "Separation zone at open channel junctions." Journal of Hydraulic Engineering. ASCE, Vol. 110, no. 11, pp.1588-1594.

Chong, N.B. (2006), "Numerical simulation of supercritical flow in open channel.", M.S.C thesis, University Technology Malaysia.

FLUENT user's guide manual-version 6.1., Fluent Incorporated, N.H., 2003.

Huang, J., Weber, L.J., Lai, Y.G. (2002), "Three dimensional numerical study of flows in open channel junctions.", Journal of Hydraulic Engineering. ASCE, Vol.128, no.3, pp.268-280.

Mao, Z. and Rong, W. (2003), "Numerical simulation of open-channel flow in 90-degree combining junction.", Journal of Tsinchua Science and Technology, Vol.8, no.6, pp.713-718.

Neary, V.S. and Odgaard, A.J. (1993), "Three dimensional flow structure at open-channel diversions. ", Journal of Hydraulic Engineering. ASCE, Vol.119, no.11, pp.1223- 1230.

Pirzadeh, B. and Shamloo, H. (2007), "Numerical investigation of velocity field in dividing open channel flow." Proceedings of the 12th WSEAS International Conference on applied mathematics, Cairo, Egypt, Desember29-31, 2007, pp.194-198.

Rodi, W. (1984), " Turbulence models and their applications in hydraulics̃A State of the Art Review", IAHR, The Netherlands.

Rodi, W. (1993), "Turbulence models and their application in hydraulics.", IAHR, Delft, The Netherlands.

Shamloo, H. and Pirzadeh, B. (2007), "Investigation of characteristics of separation zones in T-Junctions.", Proceedings of the 12th WSEAS International Conference on applied mathematics, Cairo, Egypt, Desember29-31, 2007,pp.189-193.

Taylor, E.H. (1944), "Flow characteristics at rectangular open-channel junctions. ", Transactions, ASCE, Vol.109, pp. 893–902.

Weber, L. J., Schumate, E. D., and Mawer, N. (2001), " Experiments on flow at a 90◦ open-channel junction.", Journal of Hydraulic Engineering, ASCE, Vol. 127, no. 5, pp. 340-350.

Weerakoon, S. B., Kawahara, Y. and Tamai, N. (1991), "Three-dimensional flow structure in channel confluences of rectangular section.", International Association for Hydraulic Research, A, pp.373-380.

William, L. Hays, (1980)," Statistics", third edition, P.539.

Table1: Flows tested

Qm(m^3/s)	Qb(m^3/s)	Qt(m^3/s)	q*=Qm/Qt
0.014	0.156	0.170	0.083
0.042	0.127	0.170	0.250
0.071	0.099	0.170	0.420
0.099	0.071	0.170	0.583
0.127	0.042	0.170	0.750
0.156	0.014	0.170	0.920

Table2: Chi-square test

q*	**X***	**Correlation coefficient**	**(χ^2) calculated**	**(χ^2_α) Tabulated use $\alpha = 0.05$**	**(χ^2_α) Tabulated use $\alpha = 0.1$**
0.42	-1	0.926	0.181	15.507	13.361
	-2	0.983	0.176	15.507	13.361
	-3	0.995	1.352	15.507	13.361
	-4	0.969	0.231	12.591	10.644
	-5	0.989	0.051	12.591	10.644
0.75	-1	0.959	0.566	15.507	13.361
	-2	0.995	0.323	15.507	13.361
	-3	0.987	0.214	15.507	13.361
	-4	0.994	0.110	12.591	10.644
	-5	0.984	0.125	12.591	10.644

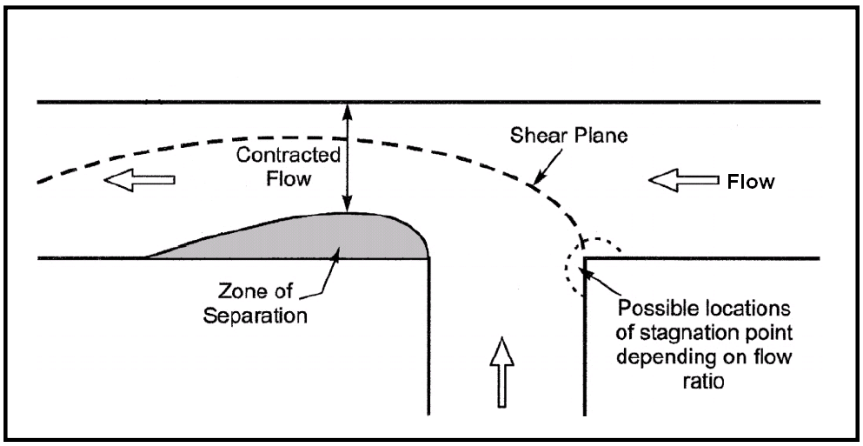

Figure1. Flow characteristics in open channel junction

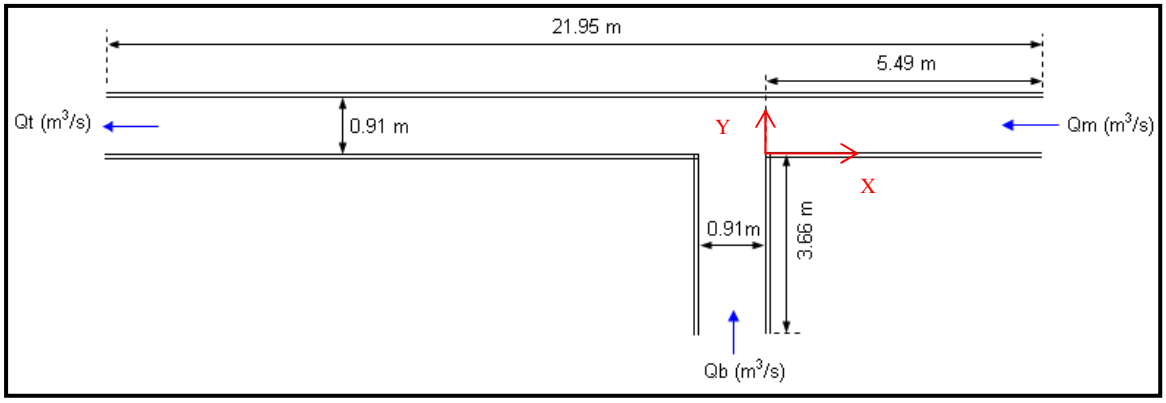

Figure 2.Plan view of test facility 90º junction

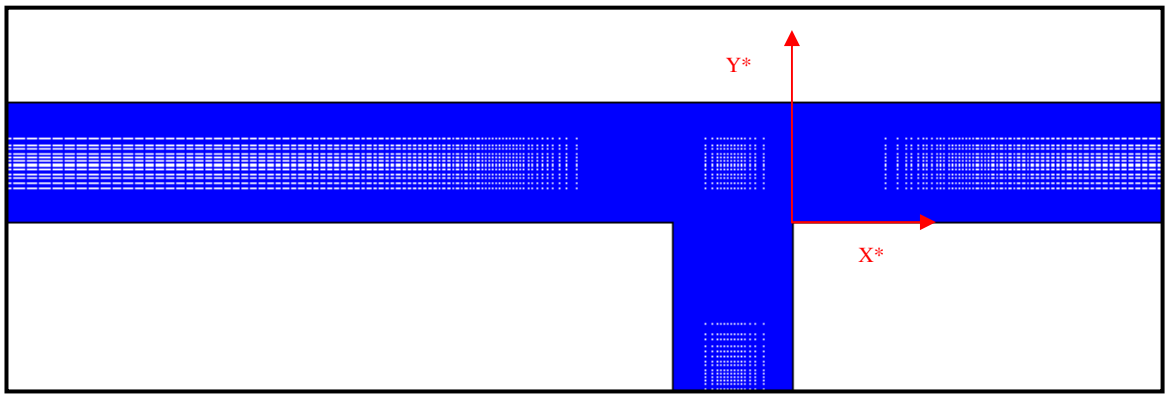

Figure 3.Computational geometry and grid.

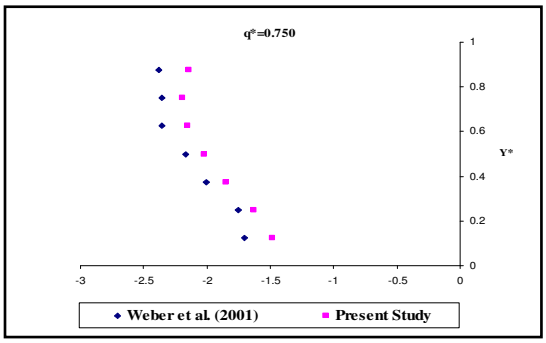

Fig.4.X-Velocity profile in the main channel(X*=-6)

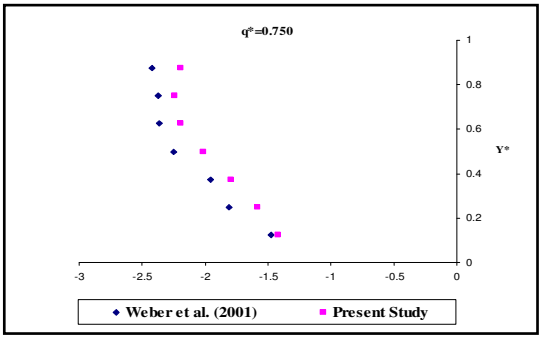

Fig.٥.X-Velocity profile in the main channel(X*=-5)

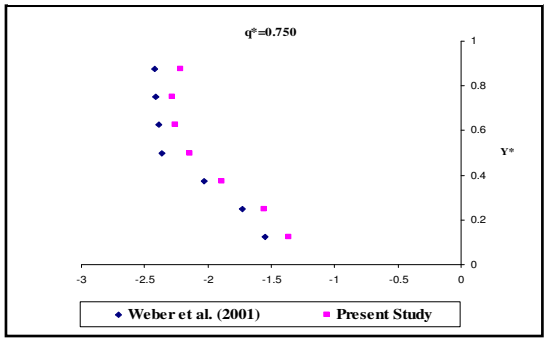

Fig.٦.X-Velocity profile in the main channel(X*=-4)

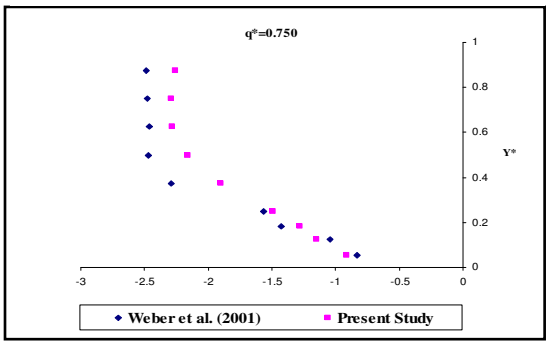

Fig.٧.X-Velocity profile in the main channel(X*=-3)

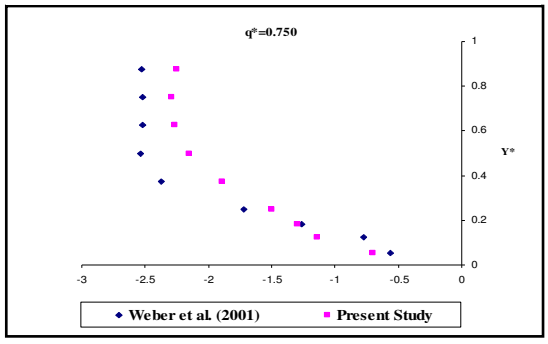

Fig.٨.X-Velocity profile in the main channel(X*=-2.67)

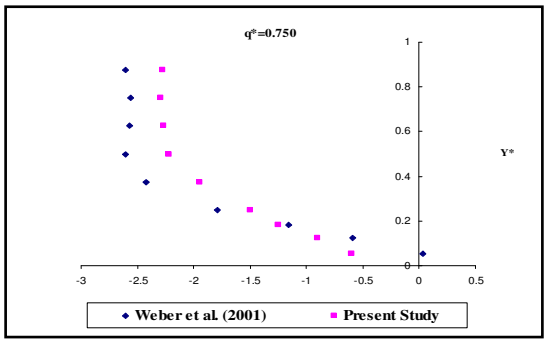

Fig.9.X-Velocity profile in the main channel(X*=-2.34)

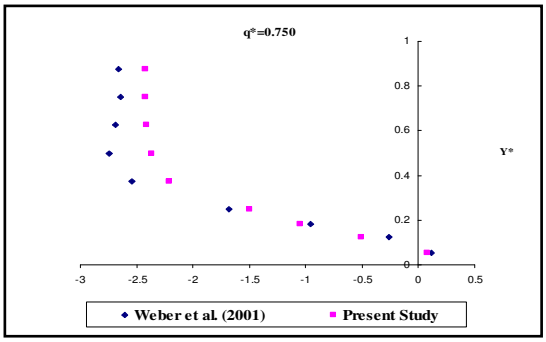

Fig.10.X-Velocity profile in the main channel(X*=-2)

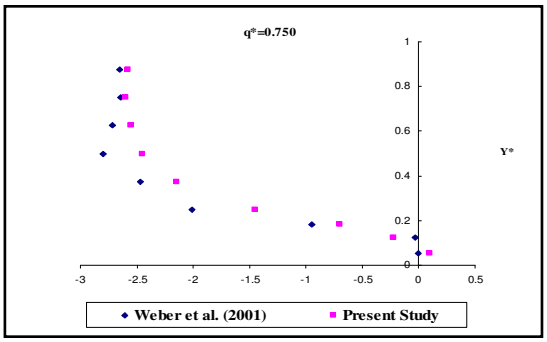

Fig.11.X-Velocity profile in the main channel(X*=-1.67)

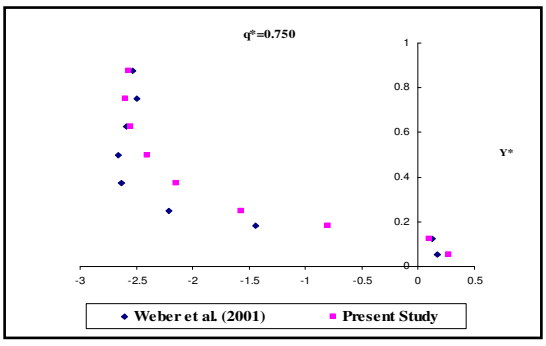

Fig.12.X-Velocity profile in the main channel(X*=-1.34)

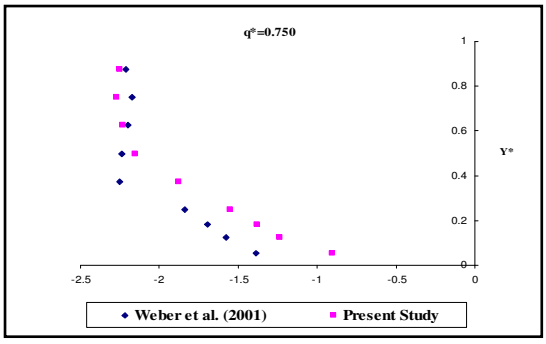

Fig.13.X-Velocity profile in the main channel(X*=-1)

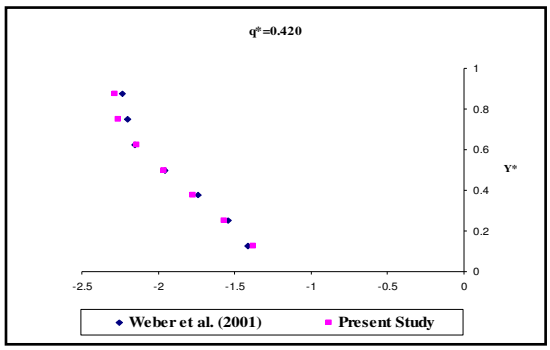

Fig.14.X-Velocity profile in the main channel (X*=-6)

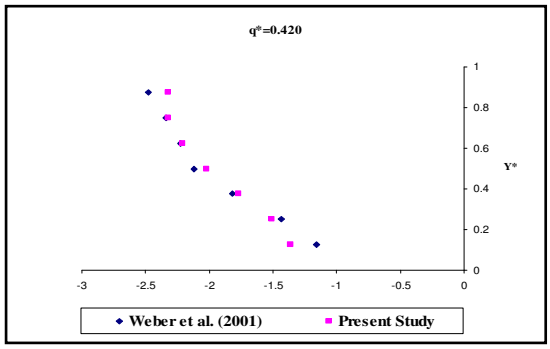

Fig.15.X-Velocity profile in the main channel (X*=-5)

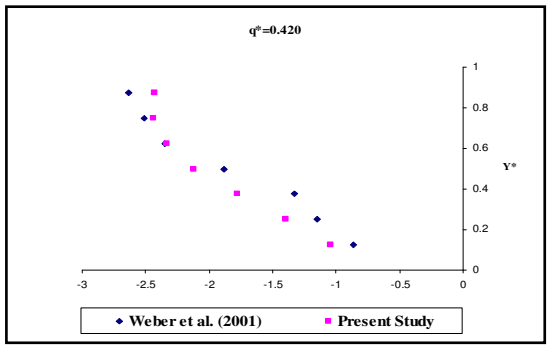

Fig.16.X-Velocity profile in the main channel (X*=-4)

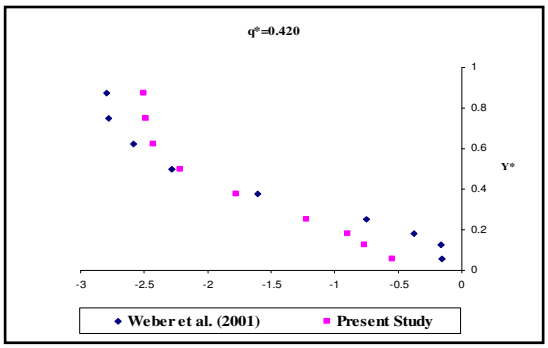

Fig.17.X-Velocity profile in the main channel (X*=-3)

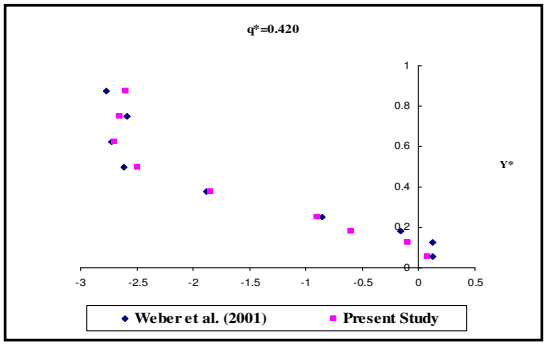

Fig.18.X-Velocity profile in the main channel (X*=-2.67)

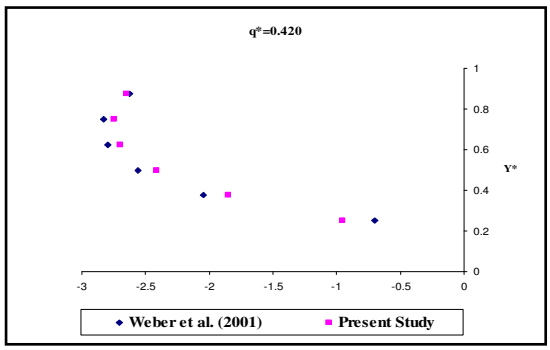

Fig.19.X-Velocity profile in the main channel (X*=-2.34)

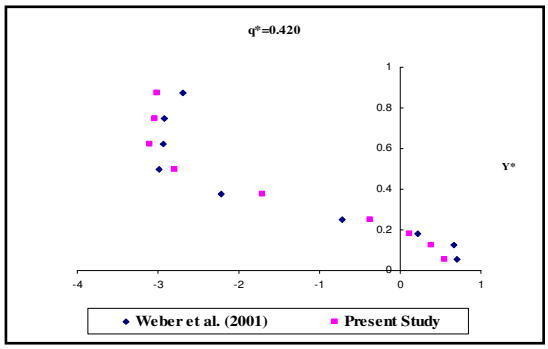

Fig.20.X-Velocity profile in the main channel (X*=-2)

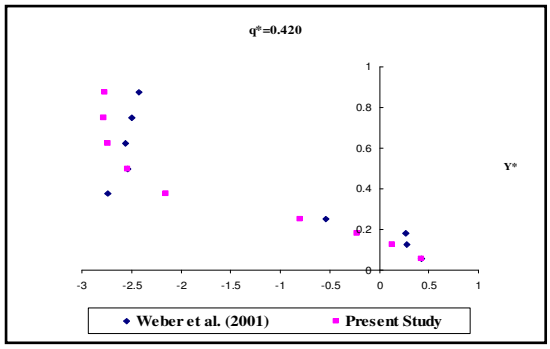

Fig.21.X-Velocity profile in the main channel (X*=-1.67)

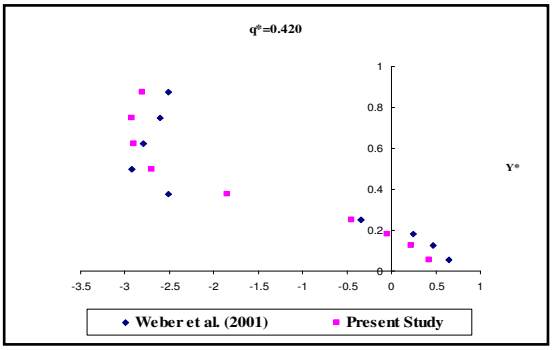

Fig.22.X-Velocity profile in the main channel (X*=-1.34)

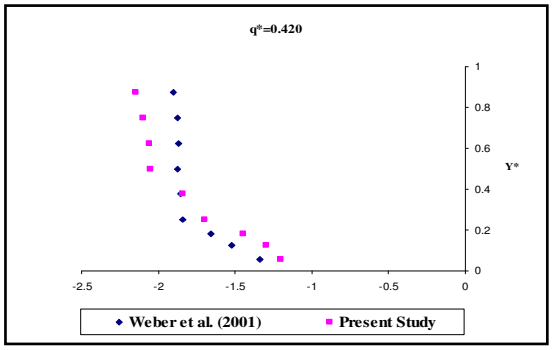

Fig.23.X-Velocity profile in the main channel (X*=-1)

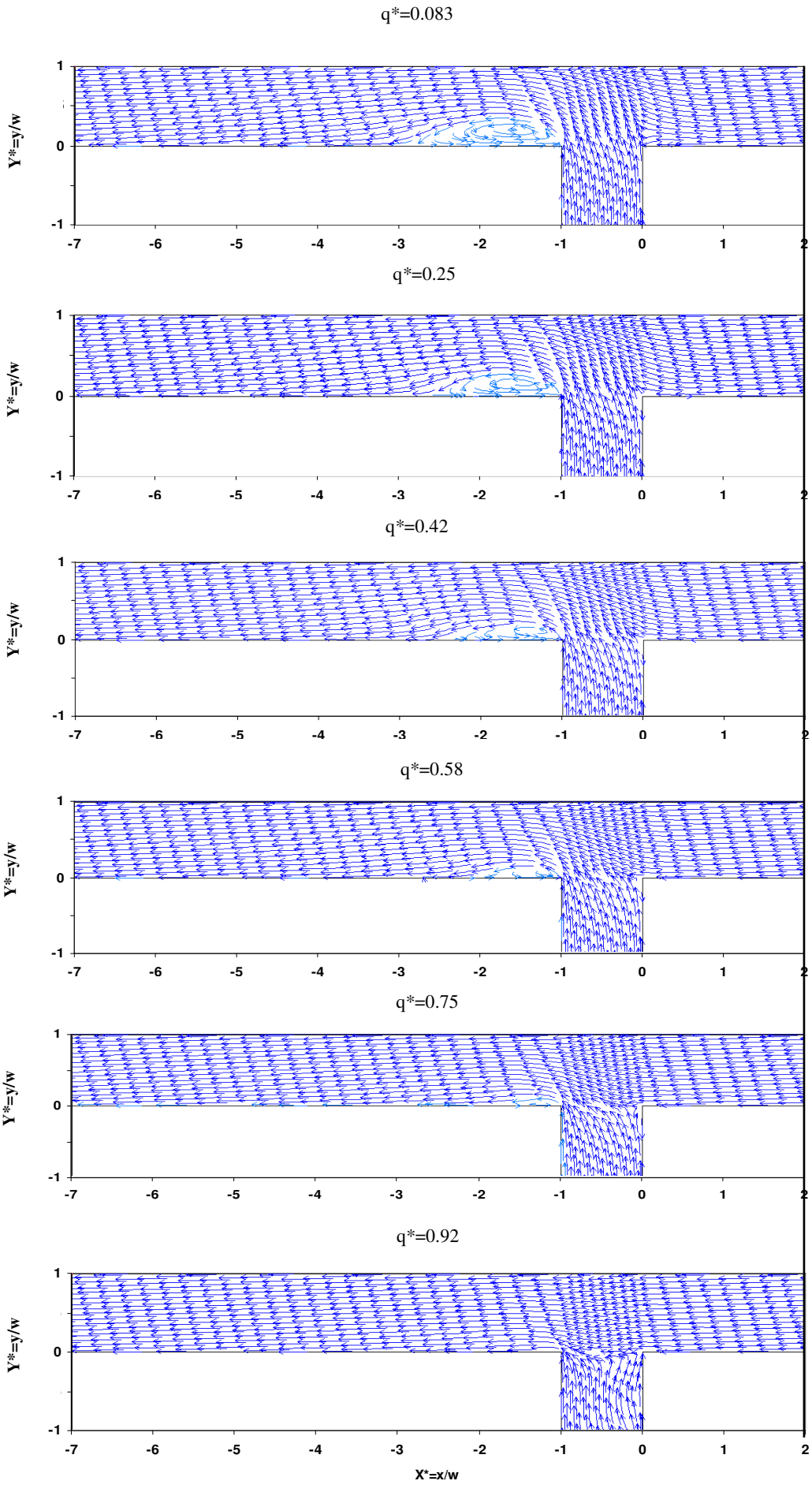

Figure 24. 2D-Streamlines plot for different discharge ratios (q*).

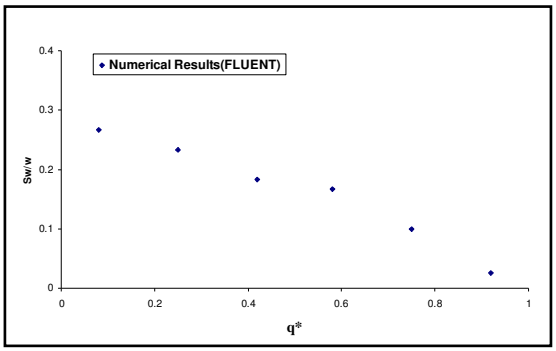

Fig.25.Dimensionless width separation zone with discharge ratio

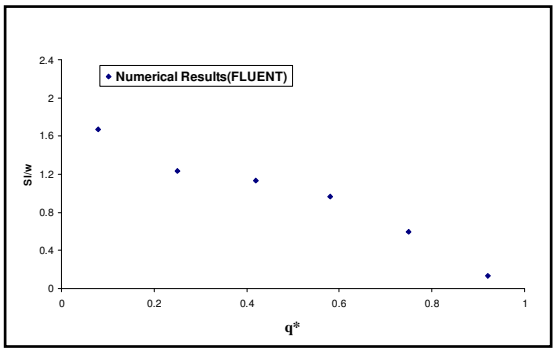

Fig.26.Dimensionless length separation zone with discharge ratio

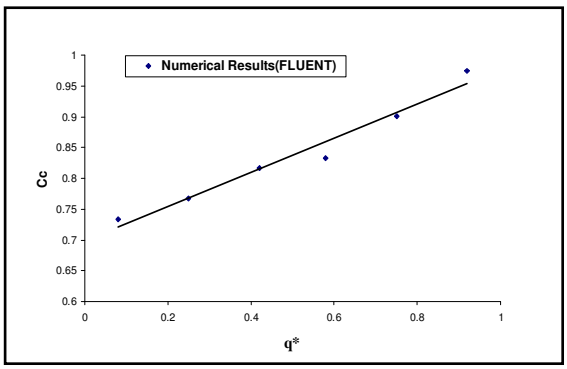

Fig.27.Contraction coefficient in D/S main channel with discharge ratio

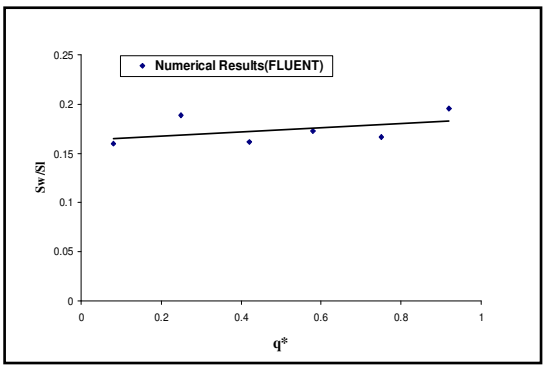

Fig.28.The ratio of Dimensionless width/length of separation zone with discharge ratio

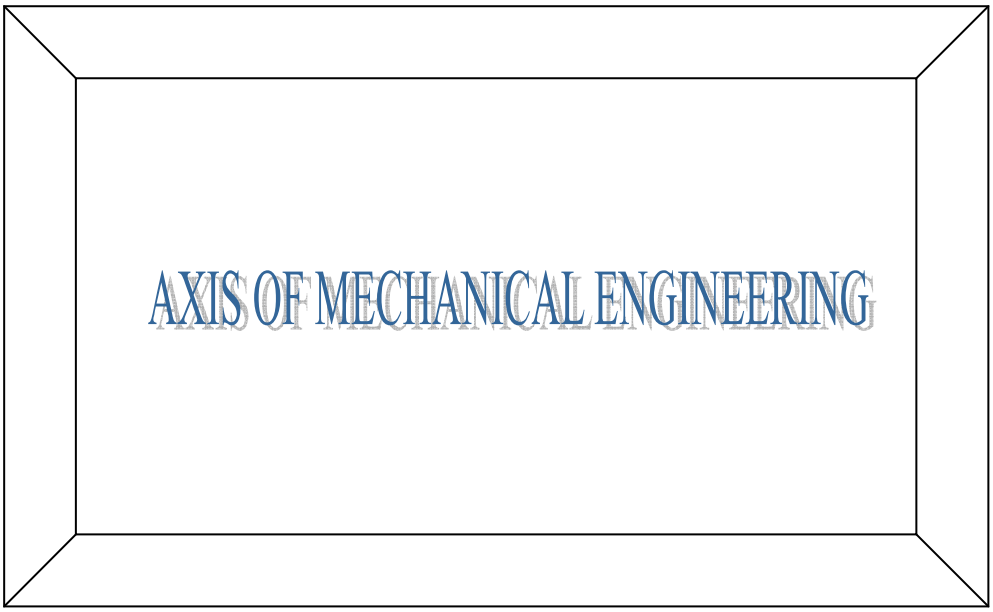
AXIS OF MECHANICAL ENGINEERING